

## Article

# The Effect of Wet and Dry Cycles on the Strength and the Surface Characteristics of Coromandel Lacquer Coatings

Wenjia Liu <sup>1,2</sup> , Ling Zhu <sup>1,2</sup>, Anca Maria Varodi <sup>3</sup>, Xinyou Liu <sup>1,2,3,\*</sup>  and Jiufang Lv <sup>1,2,\*</sup>

<sup>1</sup> College of Furnishing and Industrial Design, Nanjing Forestry University, Nanjing 210037, China; liuwenjia@hotmai.com (W.L.); zlwaxing@njfu.edu.cn (L.Z.)

<sup>2</sup> Co-Innovation Center of Efficient Processing and Utilization of Forest Resources, Nanjing Forestry University, Nanjing 210037, China

<sup>3</sup> Faculty of Furniture Design and Wood Engineering, Transilvania University of Brasov, 500036 Brasov, Romania; anca.varodi@unitbv.ro

\* Correspondence: liu.xinyou@njfu.edu.cn (X.L.); lvjiufang8189@njfu.edu.cn (J.L.); Tel.: +86-25-8542-7408 (X.L.)

**Abstract:** Research on the degradation mechanism of coating materials is crucial for the preservation of cultural heritage. The purpose of this study was to evaluate the protective effect of Coromandel coatings on wooden substrates by analyzing their dimensions, weight, adhesion strength, hydrophobicity, and glossiness. The results indicate that after five cycles, the radial moisture expansion rate of the wood specimen is 0.332%, while that of the lacquer specimen is 0.079%, representing 23.8% of the radial moisture expansion rate of untreated wood specimens. This performance is superior to that of the ash and pigment specimens. Across different experimental conditions, the change in the mass of the Coromandel specimens aligns with the trend in their dimensional changes, indicating that moisture absorption and desorption are the primary reasons for dimensional changes. The influence of temperature on mass and dimensional stability is significant only in terms of dry shrinkage rate. After wet and dry cycles at 40 °C, the adhesion strength of the Coromandel specimens decreases the most, with the ash specimens decreasing by 7.2%, the lacquer specimens by 3.2%, and the pigment specimens by 4.5%. Following wet and dry cycles at three different temperatures, the contact angle of the lacquer layers changes by less than 5%, with their contact angle values exceeding 120°. These data indicate that among the Coromandel coatings, the lacquer layer provides the best protection for the wooden substrate, while the ash coating is the most fragile. The degradation rate of the Coromandel specimens increases with rising temperatures. These findings emphasize the critical roles of humidity and temperature in protecting wooden coatings and aim to provide theoretical insights and practical significance for the preservation of wooden artifacts and the assessment of coating performance.

**Keywords:** wet and dry cycles; lacquer coating; dimensional stability; adhesion



**Citation:** Liu, W.; Zhu, L.; Varodi, A.M.; Liu, X.; Lv, J. The Effect of Wet and Dry Cycles on the Strength and the Surface Characteristics of Coromandel Lacquer Coatings. *Forests* **2024**, *15*, 770. <https://doi.org/10.3390/f15050770>

Academic Editor: Anuj Kumar

Received: 18 March 2024

Revised: 23 April 2024

Accepted: 25 April 2024

Published: 27 April 2024



**Copyright:** © 2024 by the authors. Licensee MDPI, Basel, Switzerland. This article is an open access article distributed under the terms and conditions of the Creative Commons Attribution (CC BY) license (<https://creativecommons.org/licenses/by/4.0/>).

## 1. Introduction

The history of Chinese lacquer painting in China spans over 8000 years [1,2], serving as a profound symbol of Chinese civilization. As documented in the “Record of Painting and Decorating” and interpreted by relevant experts [3–5], Coromandel lacquer involves a meticulous process. This includes applying an ash base onto wooden surfaces, coating it with black lacquer, intricately carving and selectively removing lacquer layers, and filling them with vibrant pigments to create colorful and intricate patterns. This technique flourished during the Ming and Qing dynasties, with its works commonly found on screens and other artifacts. The term “Coromandel” derives from the export of such artistry along the southeastern coast of India [6–8].

Based on the documented evidence and examination of heritage artifacts, as illustrated in Figure 1, the structure of Coromandel lacquer can be summarized as comprising

wood layers, ground layers (ash layers), lacquer layers, and pigment layers. Compared to other lacquer layer structures, the composition of Coromandel lacquer layers is more diverse, with the ground layer being relatively soft, easy to carve and decorate, and cost-effective. However, precisely because of this, the adhesion of Coromandel lacquer layers is lower. In heritage artifacts, issues such as cracking and peeling of Coromandel lacquer coatings often occur, closely linked to the environmental conditions [9]. Specifically, when rainy days are followed by sunny weather, as the humidity decreases, the moisture within the coatings permeates and evaporates, causing the coating material to contract [10,11]. This affects the cohesion between the wood, ash layers, lacquer, and pigment coatings, resulting in cracking or peeling. This phenomenon is attributed to the hygroscopic nature of wood's chemical components and the plasticity of the capillary system, leading to deformations, cracks, and a significant decrease in various strength indicators of the wood [12–14]. Repeated cycles of wetting and drying further exacerbate these issues, causing a greater decrease in wood's strength indicators and affecting its fundamental properties and functionality [15,16]. The phenomenon of hygroscopic aging explains how repeated wet and dry cycles reduce wood's hygroscopicity, reflected in dimensional changes, indicating the loss of a hygroscopic reaction after the weakening of the wood's cell wall polarity [17]. Even repair materials like glutinous rice pulp lime mortar undergo slight irreversible dimensional changes under wet and dry cycling [18].

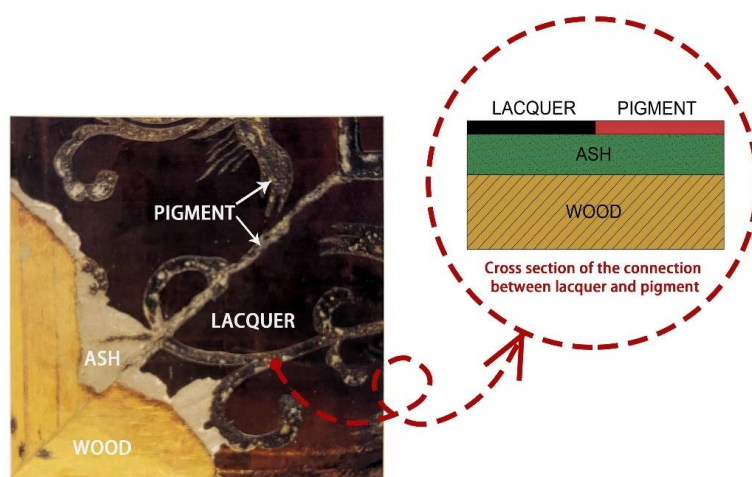


**Figure 1.** Structure diagram of damaged Coromandel screen [19].

The method of using wet and dry cycles and temperature to accelerate aging can reflect the influence of moisture on wood. Research indicates that during wet and dry cycles, wood undergoes minimal chemical changes [20]. However, repeated wet and dry cycles can cause aging effects on wood [21,22]. The commonly used wood wet and dry cycling aging conditions refer to standards such as ASTM G154 and ASTM D1037 [23,24], involving methods like immersion in water, drying, or wet and dry cycling at room temperature [25,26]. Studies have employed five cycles of alternating aging using a temperature of 50 °C and a relative humidity of 90%, establishing a relationship between moisture absorption and the aging dimensions. Additionally, research has explored the correlation between the radial and tangential shrinkage rates of wood and its thermal conductivities. Furthermore, the use of wet and dry cycles involving immersion in water and subsequent drying has been employed to verify changes in the dimensional stability of thermally modified wood. These studies collectively demonstrate that wet and dry cycles are the primary factors causing changes in the dimensional stability and moisture absorption of wood.

Surface coatings on wood exert a restraining effect on its swelling and shrinking due to moisture. This occurs because these coatings encapsulate the surface of the wood fibers, minimizing their direct exposure to moisture-laden air [10,27,28]. However, research on the changes in coating properties using wet and dry cycling methods is limited. This limi-

tation arises from the complexity of factors influencing surface coatings, which extend beyond humidity and drying conditions to include factors such as light exposure and chemical erosion. In contrast to the development of new materials, research on material degradation in cultural heritage aims to identify weaknesses in the traditional materials and the environmental factors causing material deterioration. This research aims to effectively reduce the damage caused by environmental factors to cultural heritage and to undertake targeted repair and preservation efforts.

In this study, wooden specimens, ash specimens, lacquer specimens, and pigment specimens were prepared according to the traditional processes. Artificial wet and dry cycles were induced using saturated solutions to control humidity and heating in an oven. After five wet and dry cycles, changes in the longitudinal and radial dry shrinkage rates, weight change rates, glossiness, contact angle, adhesion, and other values of the four specimens were measured systematically. The influence of the wet and dry cycle conditions on the wood substrate coatings was comprehensively investigated to provide data for studying the aging of Coromandel lacquer coating and similar coatings, offering valuable insights for the protection and restoration of relevant artifacts.

## 2. Materials and Methods

### 2.1. Materials

The raw lacquer was derived from the sap of a Chinese lacquer tree (*Toxicodendron vernicifluum* (Stokes) F. A. Barkley) located in Maoba, Hubei Province, China, and was procured from the Yangzhou Lacquerware Factory. To shorten the curing time of the raw lacquer, a refinement process was executed, following the guidelines established in the existing literature [29]. Ferrous hydroxide was prepared within the paint laboratory at Nanjing Forestry University. The natural mineral pigment ochre ( $\text{Fe}_2\text{O}_3$  in chemical composition) was sourced from Lin Shan Tang, Suzhou. Tung oil was obtained from a retailer in Nanjing. Furthermore, pig's blood was acquired from the Yangzhou Lacquerware Factory. This material was concocted by blending fresh pig's blood with a small quantity of lime and water, resulting in a gelatinous pig blood substance. This substance was subsequently utilized as a binding agent for the ground layer [30].

The Chinese fir wood (*Cunninghamia lanceolata* (Lamb.) Hook.) was purchased from Zhejiang Jeson Wood products Co., Ltd. (Huzhou, China) and possessed a moisture content of  $10 \pm 2\%$ . The wood was then cut into 96 pieces of diameter-cut boards measuring 100 (longitudinal)  $\times$  100 (radial)  $\times$  10 (tangential) mm each. These boards underwent sanding using 400# sandpaper and were conditioned within an artificial climate chamber at  $(20 \pm 2)^\circ\text{C}$  and  $(55 \pm 5)\%$  relative humidity until reaching a consistent weight, a process that spanned 14 days, before being readied for specimen preparation.

### 2.2. Material Preparation for the Black Lacquer and Oil Pigment

Drawing insights from both Xiu Shi Lu and pertinent research, the customary additive utilized in the formulation of black lacquer is generally ferrous hydroxide [4,31]. However, due to its susceptibility to oxidation in the presence of air, the preservation of ferrous hydroxide poses a challenge [32]. To ensure its efficacy, ferrous hydroxide is derived from the reaction between ferrous sulfate and sodium bicarbonate, as depicted using the chemical equation:



The amalgamation of 1 mol of  $\text{FeSO}_4$  solution with 2 mol of  $\text{NaHCO}_3$  solution results in the formation of a precipitate,  $\text{Fe}(\text{OH})_2$ . This substance takes the form of a finely textured paste, obtainable using a filtration process. Gradually, the  $\text{Fe}(\text{OH})_2$  paste is incorporated into the refined raw lacquer at a mass ratio of 20%, with thorough agitation yielding the desired black lacquer.

Furthermore, ochre powder and Tung oil are meticulously blended at a 1:1 mass ratio to create Tung oil pigment [33], ensuring an even distribution through thorough stirring.

### 2.3. Preparation of the Coromandel Specimens

Within the framework of traditional Chinese finishing techniques, the incorporation of a ground base layer between the lacquer and the wood is a customary practice aimed at enhancing the lacquer's environmental stability [19,34]. Three distinct pig blood putties were concocted by blending gel-like pig blood with three varieties of tile ash, classified by their coarseness (80-mesh for coarse ash, 100-mesh for medium ash, and 120-mesh for fine ash [35]). This blending was achieved at a 1:1 ratio. Subsequently, the fir specimens were consecutively coated with the coarse putty, followed by the medium putty, and eventually the fine putty. Each layer of putty underwent a drying period of 7 days. The cumulative thickness of these three putty layers was approximately 1 mm. The base putty layer serves as a transitional structure that bridges the gap between the substrate and the painted layer. This layer mends any gaps in the substrate, safeguards it, and prevents paint moisture from permeating into the wood, thereby averting wood deformation [19]. Concurrently, it ensures a seamless surface, priming it for the final finish. Eventually, the wood specimens underwent sanding with 400# sandpaper. A total of 72 pig's blood–ash specimens were meticulously prepared.

For the specimens coated with the ground base layer of pig's blood and ash, a layer of black lacquer was uniformly applied to their surface. These painted specimens were then placed within a climatic chamber set at 15–20 °C and 70–85% relative humidity for over 21 days to facilitate drying. The outcome was 24 black lacquer specimens. As for the oil pigment application, it was evenly administered onto the surface of the specimens coated with the pig blood ground layer. Subsequently, these specimens were placed in a climate chamber maintained at 15–20 °C and 60–65% RH, allowing them to dry for a span surpassing two weeks. This process yielded a set of 24 oil pigment specimens.

### 2.4. Wet and Dry Cycles

The 96 specimens were categorized based on their distinct specimen structures and experimental parameters, detailed in Table 1. Out of these, each set of 24 specimens featured 6 as the control group, while the remaining 18 underwent the wet and dry cycle experiment. These 18 specimens were further divided into three subgroups, each placed within an oven at temperatures of 40 °C, 30 °C, and 20 °C, while maintaining a temperature fluctuation of  $\pm 2$  °C. Within each temperature subgroup, there were 6 wood specimens, 6 ash specimens, 6 black lacquer specimens, and 6 oil pigment specimens. To replicate the desired humidity conditions, a desiccator was employed in conjunction with a saturated magnesium chloride hexahydrate solution for the dry cycle, maintaining humidity levels between 30 and 33%. Similarly, the wet cycle utilized a saturated potassium chloride solution, maintaining humidity levels within the range of 80–85%. The experimental procedure consisted of initially subjecting the specimens to wet cycle conditions for a duration of 7 days, followed by a transition to dry cycle conditions for another 7 days. This complete sequence constitutes a singular wet and dry cycle, and this entire process was iterated for a total of 5 cycles. A visual representation of the flow of the wet and dry cycle experiments is presented in Figure 2.

**Table 1.** Design of various specimen codes, additives, and experimental conditions.

Code	Specimen Name	Specimen Structure	Temperature	Number of Specimens
W40	Wood specimen	wood	40 °C	6
W30	Wood specimen	wood	30 °C	6
W20	Wood specimen	wood	20 °C	6
W + A40	Ash specimen	wood + ash	40 °C	6
W + A30	Ash specimen	wood + ash	30 °C	6
W + A20	Ash specimen	wood + ash	20 °C	6

Table 1. Cont.

Code	Specimen Name	Specimen Structure	Temperature	Number of Specimens
W + A + L40	Lacquer specimen	wood + ash + lacquer	40 °C	6
W + A + L30	Lacquer specimen	wood + ash + lacquer	30 °C	6
W + A + L20	Lacquer specimen	wood + ash + lacquer	20 °C	6
W + A + P40	Pigment specimen	wood + ash + pigment	40 °C	6
W + A + P30	Pigment specimen	wood + ash + pigment	30 °C	6
W + A + P20	Pigment specimen </td <td>wood + ash + pigment</td> <td>20 °C</td> <td>6</td>	wood + ash + pigment	20 °C	6

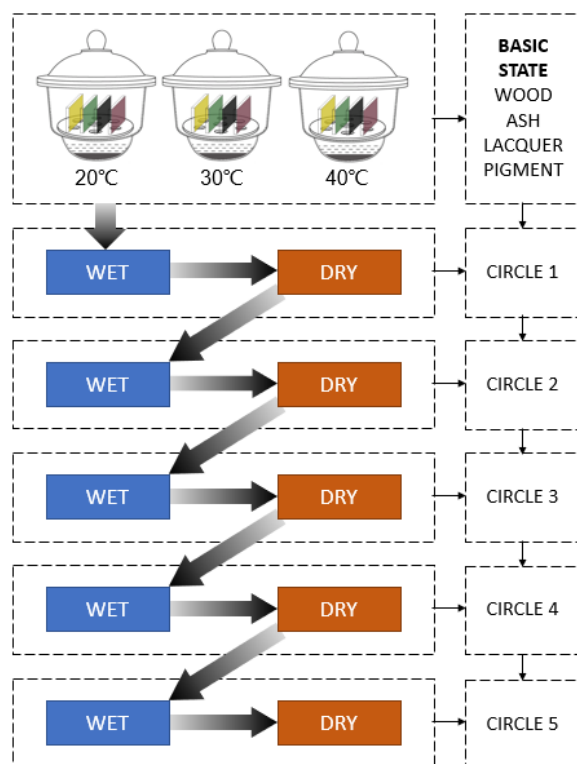


Figure 2. Flow chart of wet and dry cycle experiment.

### 2.5. Physical Tests

The tangible outcome of moisture absorption and release in Coromandel coatings is the alteration of the specimen's mass and dimensions. The practice of measuring these attributes before and during distinct cycles effectively captures the influence of wet and dry cycle conditions on a specimen's dimensions and their temporal trends. To this end, reference was made to the GB/T 1927.4-2021 standards titled "Test Method for Physical and Mechanical Properties of Small Clear Wood Specimens, Part 8: Determination of Wet Swelling" and "Test Method for Physical and Mechanical Properties of Small Clear Wood Specimens, Part 6: Determination of Dry Shrinkage" [36]. For measurement purposes, vernier calipers were utilized to assess the specimens' dimensions, while electronic balance scales were employed to gauge the specimens' weights.

The equations for determining the rates of longitudinal and radial wet swelling as well as dry shrinkage are as follows:

$$\alpha_l = \frac{L_{li} - L_{l0}}{L_{l0}} \times 100\% \quad (1)$$

$$\alpha_r = \frac{L_{ri} - L_{r0}}{L_{r0}} \times 100\% \quad (2)$$

In these formulas,  $\alpha_l$  and  $\alpha_r$  represent the wet expansion and dry shrinkage of the specimen, respectively, in both the longitudinal and radial directions, expressed as percentages.  $L_{li}$ ,  $L_{ri}$  denote the longitudinal and radial dimensions of the specimen after a single wet cycle or dry cycle, measured in millimeters (mm), while  $L_{lo}$  and  $L_{ro}$  indicate the initial longitudinal and radial dimensions of the specimen, also measured in millimeters (mm).

When both the  $\alpha_l$  and  $\alpha_r$  values are positive, the specimen undergoes wet expansion. Conversely, when both the  $\alpha_l$  and  $\alpha_r$  values are negative, the specimen experiences dry shrinkage.

Upon the specimens achieving equilibrium moisture content, the initial weight of each specimen is measured. Throughout the progression of the wet and dry cycles, the weight change rate of each specimen during one complete cycle is documented and expressed using the subsequent equation.

The equation for calculating the weight change rate [37,38] is as follows:

$$W = \frac{m - m_0}{m_0} \times 100\% \quad (3)$$

where  $W$  represents the rate of weight change, encompassing both the rate of weight decrease from high humidity to low humidity and the rate of weight increase from low humidity to high humidity, expressed as a percentage.  $m_0$  denotes the initial weight of the specimen, measured in grams (g).  $m$  signifies the weight of the specimen maintained under specific humidity conditions for a duration of 7 days, also measured in grams (g).

When the calculated value of  $W$  is positive, the specimen undergoes wet swelling. Conversely, if the calculated value of  $W$  is negative, the specimen undergoes dry shrinkage.

Subsequent to the completion of all the wet and dry cycles, the adhesion of each coating was evaluated using a BEVS adhesion meter equipped with a 20 mm diameter test column. This evaluation was conducted in accordance with the national standard "Color and Varnish Pull-off Method Adhesion Test" (GB/T 5210-2006) [39]. The aim was to identify the weakest interface within the Coromandel coating.

In accordance with the standards ASTM D523-2014 "Standard Test Method for Mirror Gloss" [40] and GBT4893.6-2013 "Physical and Chemical Properties Test of Furniture Surface Paint Film, Part 6 Gloss Determination Method" [41], a three-angle gloss meter (Guangdong San En Shi Intelligent Technology Co., Ltd., HG268, Guangdong, China) was utilized to measure the gloss of the specimens throughout the wet and dry cycles. For these measurements, the 60° angle condition was chosen. Prior to the commencement of the aging experiment and at each 7-day interval during the aging process, the glossiness data were recorded, with the same point consistently measured on the same specimen. The light loss rate of the fixed points on each test specimen was computed, and the average value yielded the light loss rate of the respective test specimen.

The formula for calculating the light loss rate is as follows:

$$H = \frac{H_0 - H_i}{H_0} \times 100\% \quad (4)$$

where  $H_0$  denotes the initial gloss, expressed as a percentage.  $H_i$  signifies the gloss after aging, expressed as a percentage.

A DSA100S droplet shape analyzer from KRUSS in Germany was employed to assess the water contact angle of the surfaces coated with Coromandel. For the testing process, the test specimen (measuring 100 × 100 mm) was subdivided into smaller 10 mm wide segments. Each coating underwent parallel testing at five distinct locations, utilizing a droplet volume of 2 μL. The initial water contact angle was recorded at each of these locations.

The core objective of this study was to illuminate the stability and aging resistance attributes of the four coatings. This was accomplished by examining the performance changes exhibited by the four Coromandel specimens across varying cycle durations and temperatures.

## 2.6. Statistical Analysis

The statistical analysis was carried out using SPSS software (IBM Corp., IBM SPSS Statistics for Windows, v. 25, Armonk, NY, USA). To assess the significant effects among different specimens and temperatures during the wet and dry cycling process, an analysis of variance (ANOVA) was executed at a significance level of 0.05. This analysis encompassed the rate of wet swelling, dry shrinkage, and weight change in the radial direction of the Coromandel specimens. Prior to conducting the one-way ANOVA tests, two essential prerequisites were addressed. The homogeneity of variance was evaluated using the Levene test, while the normal distribution of data was verified using the Shapiro–Wilk test. Both these tests were essential to establish the suitability of the data for the ANOVA. Subsequently, the mean values were distinguished using Fisher’s protected minimum significant difference (LSD) test at a significance level of  $\alpha = 0.05$ . This statistical methodology enabled the differentiation of meaningful variations among the data sets.

## 3. Results

### 3.1. Dimensional Stability

The moisture-related swelling and shrinking rates of wood are important parameters describing its dimensional changes. For Coromandel specimens using Chinese fir wood as the base material, the main source of dimensional variation lies in the fir wood itself, while the ash layer, lacquer layer, and pigment layer of the Coromandel affect it. In order to better study the dimensional stability of the Coromandel layers, the experiment first verified the longitudinal and radial dimension change rates due to the swelling and shrinking of the fir wood specimens under different temperature conditions during wet and dry cycling, as shown in Figure 3. The longitudinal wet swelling and shrinkage rates of the fir wood specimens are lower than the radial wet swelling and shrinkage rates [40,41], and the radial wet swelling and shrinkage rates are approximately ten times those of the longitudinal rates, consistent with the research findings in literature [26,42,43]. The underlying cause is attributed to the structural and fiber orientation disparities within the wood. Longitudinally oriented fibers exhibit greater stability due to their robust interconnections, resulting in minimal longitudinal shrinkage or swelling. Conversely, fibers oriented in the radial direction are comparatively weaker, featuring more fragile interconnections. Consequently, they are more susceptible to moisture-induced changes, resulting in pronounced shrinkage or swelling in the radial direction.

Throughout the aging process, the Coromandel specimens underwent five cycles of wet and dry conditions. Notably, the rate of wet and dry shrinkage exhibited a gradual reduction over time. This phenomenon can be attributed to the “moisture-absorption fatigue synthesis mechanism” intrinsic to wood. Hygroscopic aging refers to the partial loss of wood’s hygroscopic response, occurring as a consequence of a process wherein the cell wall polarity diminishes [44]. This mechanism entails a partial saturation of the cell wall polar groups, rendering them less responsive to water vapor fixation. This is reflected in the decrease in the swelling and shrinking rates observed in the experimental data, which conforms to this pattern under different temperature conditions.

The maximum longitudinal and radial wet swelling and dry shrinkage rates of the Coromandel specimens under wet and dry cycling conditions are presented in Table 2. At room temperature (20 °C), the radial wet swelling rate of 0.565% significantly exceeded the longitudinal wet swelling rate of 0.061% during the wet cycle. Similarly, the radial dry shrinkage rate of −0.292% was notably higher than the longitudinal dry shrinkage rate of −0.033% observed during the dry cycle. This discrepancy arises from the mechanism of water absorption in the longitudinal direction of wood [12,45]. In this scenario, water primarily traverses continuous pathways composed of tubular cells, driven by potent capillary forces. This facilitates rapid water transport within the wood. In contrast, when water is conveyed transversely across the wood, its movement is constrained by the necessity to navigate through grain pores, slowing down the transport process.

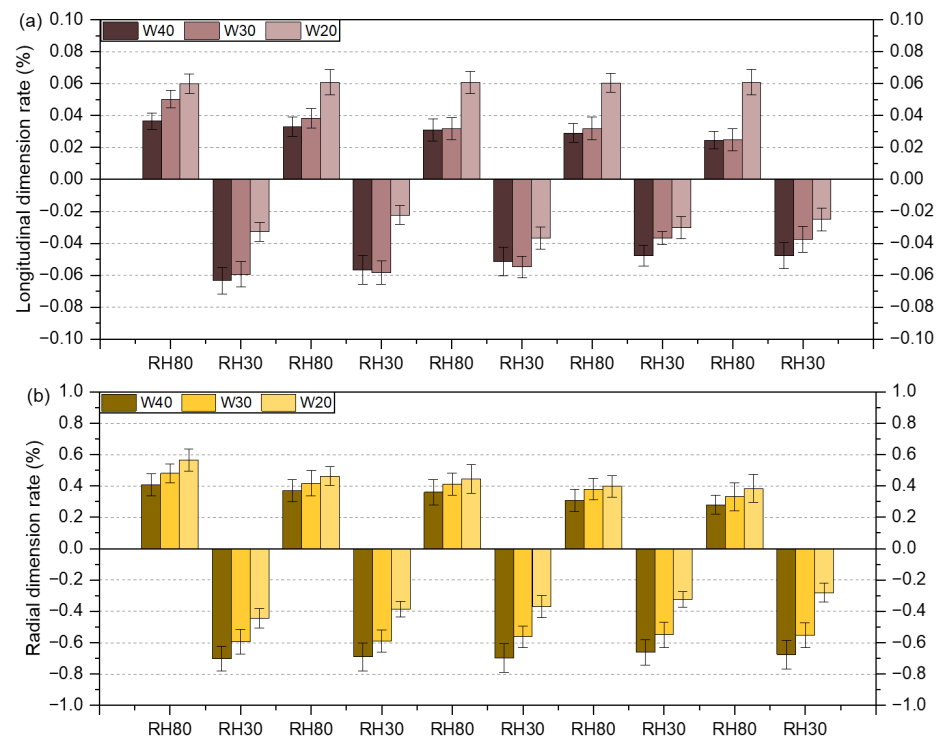


**Figure 3.** Longitudinal and radial dimension rates of the wood specimen under wet and dry cycling conditions. (a) Longitudinal dimension rate of the wood specimen; (b) radial dimension rate of the wood specimen.

**Table 2.** Maximum values of longitudinal and radial direction wet expansion and dry shrinkage of the Coromandel specimens under wet and dry cycling conditions.

e		Wood 20 °C (%)	Ash 20 °C (%)	Lacquer 20 °C (%)	Pigment 20 °C (%)
Wet circle	$\alpha_l$	0.061 ± 0.008	0.058 ± 0.012	0.049 ± 0.008	0.048 ± 0.011
	$\alpha_r$	0.565 ± 0.071	0.633 ± 0.102	0.272 ± 0.059	0.489 ± 0.064
Dry circle	$\alpha_l$	-0.037 ± 0.007	-0.051 ± 0.013	-0.050 ± 0.006	-0.046 ± 0.007
	$\alpha_r$	-0.445 ± 0.062	-0.208 ± 0.057	-0.425 ± 0.063	-0.184 ± 0.032

The ash, lacquer, and pigment specimens likewise exhibited greater radial wet and dry shrinkage rates compared to their longitudinal counterparts. Pig's blood-ash, black lacquer, and oil pigment finishes collectively influence the wet swelling and dry shrinkage behavior of the underlying fir wood base material. During the wet cycle, both the black lacquer and the oil pigment significantly curbed the wood's wet swelling. Conversely, in the dry cycle, the pig's blood-ash and oil pigment exerted significant inhibitory effects on the wood's dry shrinkage. Given that radial wet swelling and dry shrinkage are the pivotal factors contributing to the dimensional deformation of Coromandel furniture, a comprehensive analysis of the radial dimensional behavior is presented below.

The radial dimension change rates of the Coromandel specimens under wet and dry cycling conditions are shown in Table 3. In the wet cycle, the moisture absorption rate of the ash specimens is slightly higher than that of the wood specimens, while the moisture absorption rate of the pigment specimens is slightly lower than that of the wood specimens, and the moisture absorption rate of the lacquer specimens is significantly lower than that of the wood specimens. This is because in the three-layer structure of Coromandel specimens, the lacquer effectively prevents moisture from penetrating through the surface layer and the ash layer into the wood layer [46]. After five cycles, the radial moisture expansion rates for the wood specimens, ash specimens, lacquer specimens, and pigment specimens

are 0.332%, 0.427%, 0.079%, and 0.368%, respectively. The lacquer specimen notably outperforms the ash and pigment specimens, representing only 23.8% of the radial moisture expansion rate of the untreated wood specimens. The moisture expansion data on the Coromandel coatings directly reflect the dimensional changes caused by moisture absorption under natural conditions, which are particularly important. In the dry cycle, the drying rate of the wood specimens and the lacquer specimens is higher than that of the ash specimens and the pigment specimens. This is because the hygroscopic nature of the ash and pigment specimens affects the drying properties of the base wood. When the type of specimen is used as a factor, all the *p*-values are less than 0.05, indicating that the type of specimen has a significant effect on Coromandel specimens [47].

**Table 3.** Radial dimension change rate of the Coromandel specimens under wet and dry cycling conditions.

Code	Cycle1		Cycle2		Cycle3		Cycle4		Cycle5	
	Wet	Dry	Wet	Dry	Wet	Dry	Wet	Dry	Wet	Dry
Specimen type										
W	0.484 <sup>a</sup>	−0.580 <sup>b</sup>	0.417 <sup>a</sup>	−0.556 <sup>b</sup>	0.406 <sup>a</sup>	−0.542 <sup>b</sup>	0.361 <sup>a</sup>	−0.512 <sup>b</sup>	0.332 <sup>a</sup>	−0.503 <sup>b</sup>
W + A	0.507 <sup>a</sup>	−0.268 <sup>a</sup>	0.488 <sup>a</sup>	−0.258 <sup>a</sup>	0.470 <sup>a</sup>	−0.260 <sup>a</sup>	0.435 <sup>a</sup>	−0.248 <sup>a</sup>	0.427 <sup>a</sup>	−0.240 <sup>a</sup>
W + A + L	0.164 <sup>b</sup>	−0.516 <sup>b</sup>	0.120 <sup>b</sup>	−0.506 <sup>b</sup>	0.099 <sup>b</sup>	−0.499 <sup>b</sup>	0.088 <sup>b</sup>	−0.475 <sup>b</sup>	0.079 <sup>b</sup>	−0.460 <sup>b</sup>
W + A + P	0.409 <sup>a</sup>	−0.350 <sup>a</sup>	0.393 <sup>a</sup>	−0.322 <sup>a</sup>	0.383 <sup>a</sup>	−0.306 <sup>a</sup>	0.379 <sup>a</sup>	−0.274 <sup>a</sup>	0.368 <sup>a</sup>	−0.240 <sup>a</sup>
Temperature										
40 °C	0.348 <sup>a</sup>	−0.549 <sup>b</sup>	0.326 <sup>a</sup>	−0.535 <sup>c</sup>	0.313 <sup>a</sup>	−0.526 <sup>b</sup>	0.282 <sup>a</sup>	−0.495 <sup>b</sup>	0.268 <sup>a</sup>	−0.472 <sup>a</sup>
30 °C	0.375 <sup>a</sup>	−0.421 <sup>a</sup>	0.356 <sup>a</sup>	−0.406 <sup>b</sup>	0.354 <sup>a</sup>	−0.399 <sup>a</sup>	0.343 <sup>a</sup>	−0.383 <sup>ab</sup>	0.324 <sup>a</sup>	−0.375 <sup>ab</sup>
20 °C	0.450 <sup>a</sup>	−0.315 <sup>a</sup>	0.381 <sup>a</sup>	−0.291 <sup>a</sup>	0.353 <sup>a</sup>	−0.281 <sup>a</sup>	0.322 <sup>a</sup>	−0.253 <sup>a</sup>	0.313 <sup>a</sup>	−0.237 <sup>a</sup>
<i>p</i> Values										
Specimen type	<0.001	<0.001	<0.001	<0.001	<0.001	<0.001	<0.001	<0.001	<0.001	0.001
Temperature	0.267	<0.001	0.653	<0.001	0.783	<0.001	0.572	0.001	0.454	0.003
Specimen type × Temperature	0.435	0.698	0.505	0.434	0.722	0.679	0.496	0.741	0.279	0.672

Note: Mean values of H followed by the same small superscript letters (<sup>a-c</sup>) within a group are not significantly different based on Fisher’s protected LSD test at the 0.05 significance level. The *p*-value indicates the significance of the influencing factor. A smaller *p*-value indicates stronger significance. Generally, when the *p*-value is less than 0.05, the influencing factor is considered significant, and when the *p*-value is greater than 0.05, it is considered insignificant.

The moisture expansion and contraction rates of the Coromandel specimens are also influenced by different temperatures under wet and dry cycle conditions. The moisture expansion rates of the Coromandel specimens in the radial direction at different temperatures are shown in Figure 4. Under wet cycle conditions, at 40 °C, the radial moisture expansion rate of the four types of Coromandel specimens is lower than at 30 °C, which, in turn, is lower than at 20 °C. Under dry cycle conditions, at 40 °C, the radial drying shrinkage rate of the four types of Coromandel specimens is greater than at 30 °C, which, in turn, is greater than at 20 °C. Temperature promotes the drying process of the Coromandel specimens, leading to an increase in the radial drying shrinkage rate of the Coromandel specimens. Some scholars have also conducted drying under high-temperature and low-humidity conditions [48], indicating that this condition has the highest aging efficiency. Meanwhile, low temperatures are more conducive to the moisture absorption of the Coromandel specimens. It can be inferred that under conditions of a low temperature and high humidity or a high temperature and low humidity, the dimensional variation in the Coromandel coatings is maximal, and their dimensional stability is poorest. Through significance analysis, it can be observed that during the dry cycle process, the *p*-value is less than 0.05, indicating significance; however, during the wet cycle, it is not significant.

In terms of the significance analysis of the wet and dry cycles, the type of specimen wielded a significant impact on the wet swelling and dry shrinkage rates, while temperature significantly affected dry shrinkage. However, the interaction between the Coromandel specimen type and temperature was not significant. This suggests that specimen type and temperature independently influence the wet swelling and dry shrinkage rates. Consequently, when assessing and regulating these rates, considering specimen type and temperature as distinct factors, rather than focusing on their interaction, is advisable.

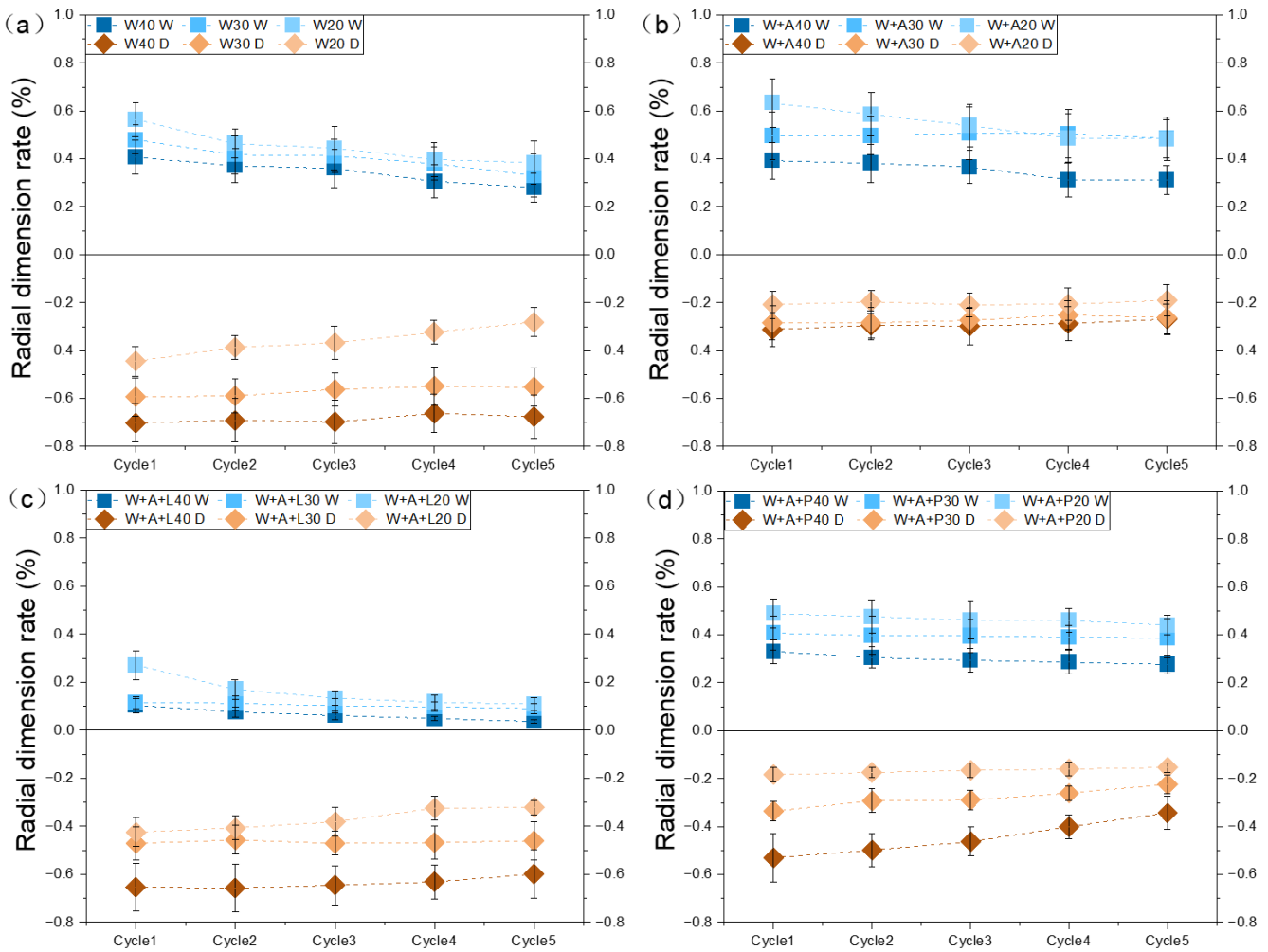


**Figure 4.** Radial dimension change rate of the Coromandel specimens at different temperatures. (a) Wood specimen; (b) ash specimen; (c) lacquer specimen; (d) pigment specimen.

### 3.2. Weight Change

The weight change rate of the Coromandel specimens under the wet and dry cycles is shown in Table 4 and Figure 5. During wet and dry cycles, changes in specimen weight are mainly due to changes in the moisture absorption and desorption of the specimens, reflecting primarily changes in the moisture absorption and desorption of the base material, fir wood, under different temperatures and wet and dry cycle conditions. Simultaneously, they reflect the effects of the ash layer, the black lacquer layer, and the oil pigment layer on the moisture absorption and desorption of the base fir wood. Under wet and cycle conditions, the quality of the Coromandel coatings fluctuates with humidity. The influence of oil pigment and ash on the moisture absorption rate of fir wood is relatively weak, but the protective effect of the black lacquer is evident. This is because the dense black lacquer blocks the exchange of moisture between the ash and the surface of the wood and the external humidity environment [49]. Under dry cycle conditions, the weight change in the wood specimens and the lacquer specimens is greater than that of the ash specimens and the pigment specimens. Regarding the influence of temperature on the Coromandel specimens, the weight change rate of the Coromandel coatings is highest at 40 °C and lowest at 20 °C. The type of specimen has a significant effect on weight change, but temperature and the interaction between specimen type and temperature are not significant. These patterns are consistent with the dimensional stability of the Coromandel specimens, indicating that moisture absorption and desorption are the primary factors influencing dimensional changes.

**Table 4.** Weight change rate of the Coromandel specimens under wet and dry cycling conditions.

Code	Cycle1		Cycle2		Cycle3		Cycle4		Cycle5	
	Wet	Dry	Wet	Dry	Wet	Dry	Wet	Dry	Wet	Dry
Specimen type										
W	2.513 <sup>a</sup>	−2.697 <sup>bc</sup>	2.421 <sup>a</sup>	−2.677 <sup>b</sup>	2.362 <sup>a</sup>	−2.692 <sup>b</sup>	2.218 <sup>a</sup>	−2.594 <sup>b</sup>	1.978 <sup>a</sup>	−2.623 <sup>c</sup>
W + A	2.262 <sup>ab</sup>	−1.843 <sup>ab</sup>	2.187 <sup>a</sup>	−1.817 <sup>a</sup>	2.188 <sup>a</sup>	−1.789 <sup>a</sup>	2.163 <sup>a</sup>	−1.671 <sup>a</sup>	2.085 <sup>a</sup>	−1.767 <sup>ab</sup>
W + A + L	1.383 <sup>b</sup>	−2.746 <sup>c</sup>	1.191 <sup>b</sup>	−2.721 <sup>b</sup>	1.020 <sup>b</sup>	−2.674 <sup>b</sup>	0.891 <sup>b</sup>	−2.578 <sup>b</sup>	0.778 <sup>b</sup>	−2.570 <sup>bc</sup>
W + A + P	2.526 <sup>a</sup>	−1.559 <sup>a</sup>	2.490 <sup>a</sup>	−1.480 <sup>a</sup>	2.389 <sup>a</sup>	−1.482 <sup>a</sup>	2.254 <sup>a</sup>	−1.417 <sup>a</sup>	2.314 <sup>a</sup>	−1.414 <sup>a</sup>
Temperature										
40 °C	1.634 <sup>a</sup>	−3.256 <sup>c</sup>	1.614 <sup>b</sup>	−3.224 <sup>c</sup>	1.586 <sup>a</sup>	−3.261 <sup>c</sup>	1.508 <sup>a</sup>	−3.160 <sup>b</sup>	1.342 <sup>a</sup>	−3.213 <sup>c</sup>
30 °C	2.212 <sup>ab</sup>	−2.401 <sup>b</sup>	2.143 <sup>ab</sup>	−2.320 <sup>b</sup>	2.040 <sup>ab</sup>	−2.266 <sup>b</sup>	1.972 <sup>a</sup>	−2.105 <sup>b</sup>	1.863 <sup>ab</sup>	−2.132 <sup>b</sup>
20 °C	2.667 <sup>a</sup>	−0.977 <sup>a</sup>	2.460 <sup>a</sup>	−0.978 <sup>a</sup>	2.344 <sup>a</sup>	−0.951 <sup>a</sup>	2.166 <sup>a</sup>	−0.931 <sup>a</sup>	2.161 <sup>a</sup>	−0.936 <sup>a</sup>
<i>p</i> Values										
Specimen type	0.009	0.002	0.002	<0.001	<0.001	0.001	0.001	<0.001	<0.001	0.001
Temperature	0.008	<0.001	0.019	<0.001	0.014	<0.001	0.088	<0.001	0.004	<0.001
Specimen type × Temperature	0.977	0.987	0.976	0.947	0.998	0.979	0.994	0.977	0.987	0.973

Note: Mean values of H followed by the same small superscript letters (<sup>a-c</sup>) within a group are not significantly different based on Fisher’s protected LSD test at the 0.05 significance level. The *p*-value indicates the significance of the influencing factor. A smaller *p*-value indicates stronger significance. Generally, when the *p*-value is less than 0.05, the influencing factor is considered significant, and when the *p*-value is greater than 0.05, it is considered insignificant.

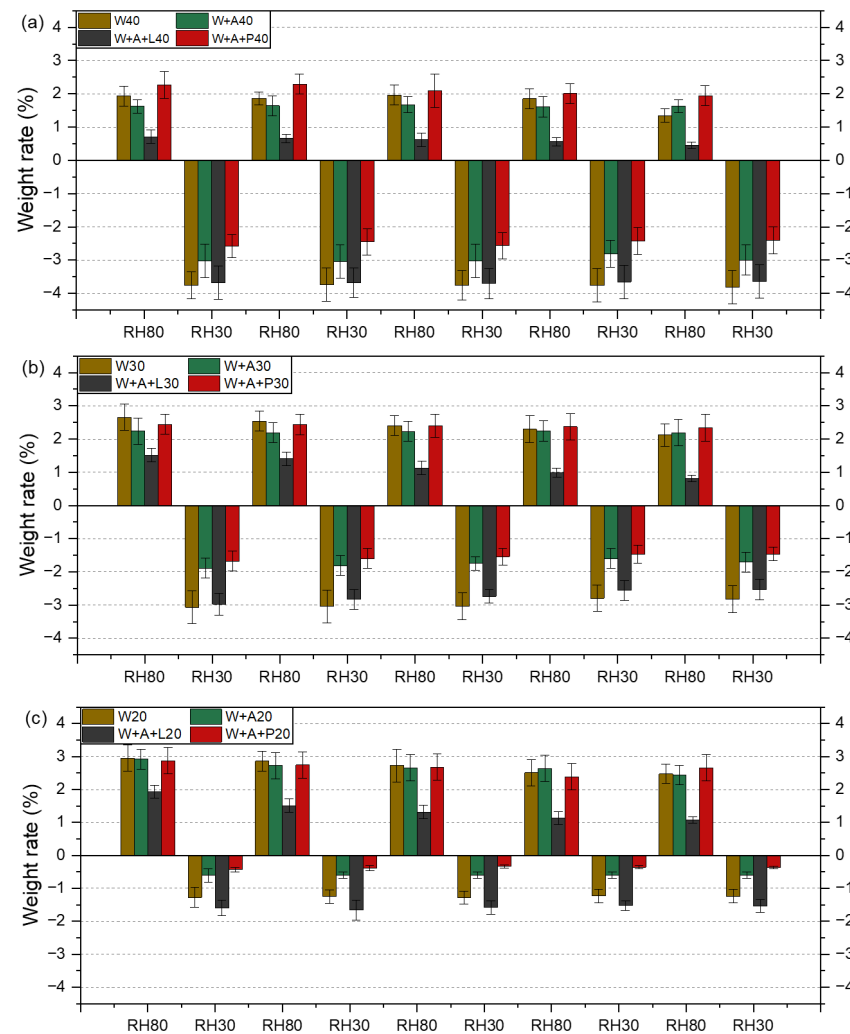


**Figure 5.** Weight change rate of the Coromandel specimens under wet and dry cycling conditions at different temperatures. (a) Weight change rate of the Coromandel specimens at 40 °C; (b) weight change rate of the Coromandel specimens at 30 °C; (c) weight change rate of the Coromandel specimens at 20 °C.

### 3.3. Adhesion

In the realm of organic coatings, the adhesion to the substrate stands as a pivotal characteristic [50]. In general, increased humidity leads to loss of the coating's material strength, as well as reduced adhesion between the wood and the coating [51]. To delve deeper into the impact of wet and dry cycles on Coromandel coatings, an evaluation of the adhesion alterations of the Coromandel specimens prior to and following the wet and dry cycles was conducted, as illustrated in Figure 6. Notably, the ash, lacquer, and pigment specimens each exhibited a marginal reduction in their adhesion after undergoing the wet and dry cycles. It is worth highlighting that the adhesion of the lacquer and pigment specimens slightly surpassed that of the ash specimen. The greatest decrease was observed at 40 °C, with the ash specimens decreasing by 7.2%, the lacquer specimens by 3.2%, and the pigment specimens by 4.5%.

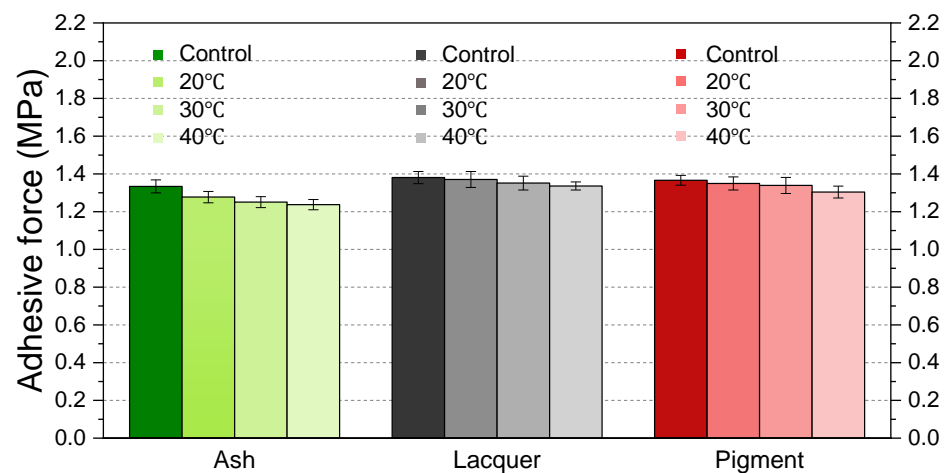


**Figure 6.** Changes in adhesion of Coromandel specimens after wet and dry cycles.

When subjected to tension, there was a fracture between the ash layer and the wood, as shown in Figure 7. Additionally, it can be observed from the figures that a small amount of the ash layer still remained on the wood substrate after the adhesion test, indicating that the mechanical strength of the ash layer itself is not high. The significant variations in the radial moisture expansion and contraction rates and the weight change rates of the ash specimens in the dimensional stability experiments also confirm this result. This suggests that the ash layer is a weak interface in Coromandel coatings, and the interface between the ash layer and the wood layer is the weakest layer.

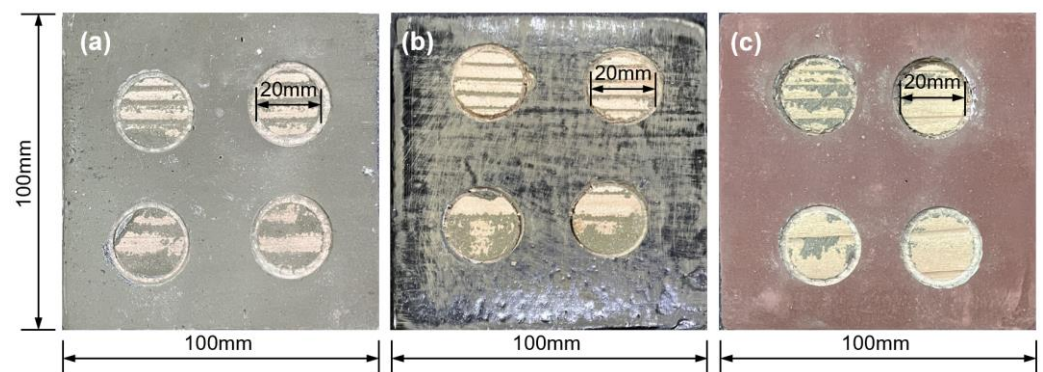


**Figure 7.** Part of Coromandel specimens after the adhesion test. (a) Ash specimen; (b) lacquer specimen; (c) pigment specimen.

The fracture of the lacquer and pigment specimens still occurs between the ash layer and the wood substrate. This is because the adhesion between the ash layer and the wood

substrate is still weaker than the adhesion between the ash layer and the lacquer or pigment layers. However, the adhesion of the lacquer and pigment specimens is higher than that of the ash specimen. This is because during the wet and dry cyclic aging process, the encapsulation of the lacquer and pigment layers partially prevents moisture from penetrating, delaying the degradation of the ash layer and wood substrate [52,53], thereby improving the adhesion to a certain extent.

### 3.4. Contact Angle

Figure 8 depicts the contact angle values of the Coromandel specimens subjected to wet and dry cycling, at the initial stage, after cycling at 20 °C, 30 °C, and 40 °C. Aging has a decreasing effect on the contact angle of the coating for all the specimens [54]. This is because the humidity variation during the cycles causes the expansion and contraction of the specimens, resulting in microscale damage on the surface, leading to an increase in the roughness of the Coromandel coatings. Liquids tend to spread more easily on rough surfaces, causing an increase in wetting and a decrease in hydrophobicity, resulting in decreased contact angle values. As the temperature during the wet and dry cycles increases, the decrease in the contact angle values becomes more pronounced. This is because temperature accelerates the aging of the specimens, further reducing their hydrophobicity.

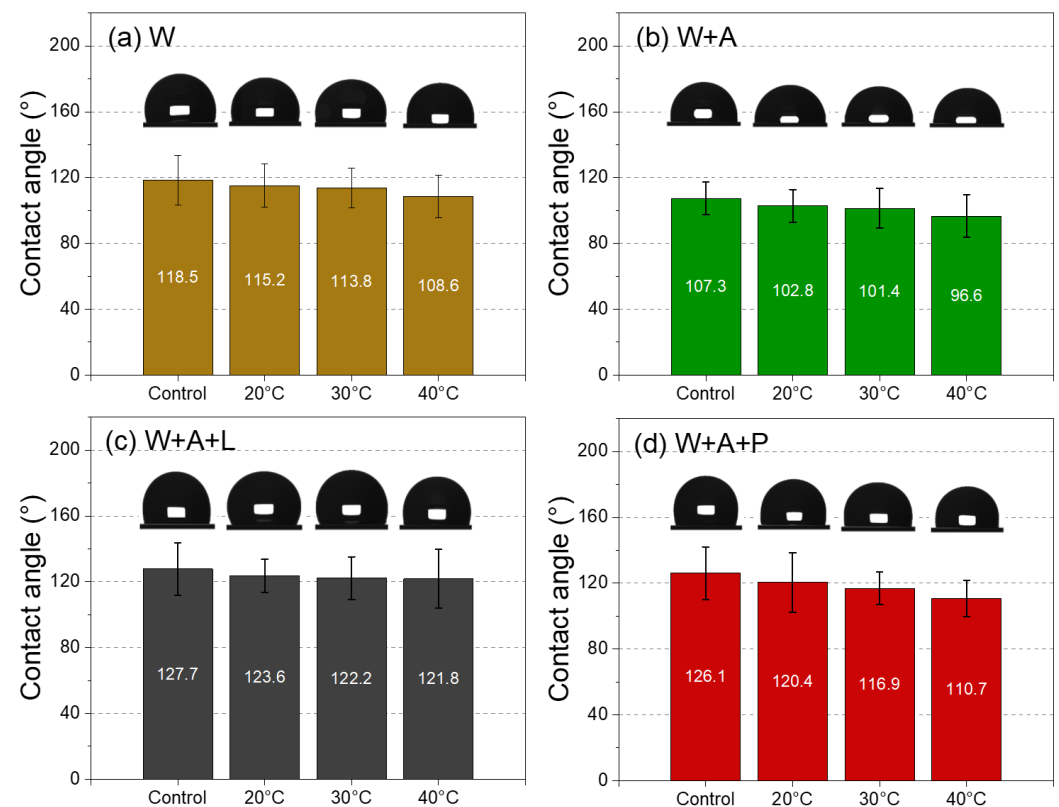


**Figure 8.** Contact angle of Coromandel specimens under wet and dry cycling conditions. (a) Wood specimen; (b) ash specimen; (c) lacquer specimen; (d) pigment specimen.

Using the contact angle values of the fir wood substrate before it underwent wet and dry cycling as a benchmark, it was observed that both the lacquer and pigment specimens exhibited higher contact angles compared to the wood specimens, while the ash specimens displayed lower contact angles. This reflects the protective effect of the lacquer and pigment coatings on the wood. After undergoing the wet and dry cycles, the contact angle values of all four types of specimens decreased. At 20 °C, the decrease rates of the wood layer, ash layer, lacquer layer, and pigment layer are 2.8%, 4.2%, 3.2%, and 4.5%, respectively; at 30 °C, the decrease rates are 4.0%, 5.5%, 4.3%, and 7.3%, respectively; at 40 °C, the decrease rates are 8.4%, 10.0%, 4.6%, and 12.2%, respectively. It can be observed that

the decrease rates of the ash and pigment layers are higher than those of the wood and lacquer layers.

The change in the contact angle of the lacquer layer is less than 5% under all three temperature conditions, and the contact angle values are greater than  $120^\circ$ . This is because the main component of lacquer, phenolic compounds, contains a benzene ring structure, which provides strong  $\pi$ - $\pi$  stacking interactions between molecules [55], forming a closely packed molecular structure on the lacquer film surface, making the surface smooth and the contact angle value high. In the oil pigment layer, the fatty acids and oleic acids of the binding agent Tung oil undergo oxidation reactions during the drying process, forming a dense cross-linked network structure [56]. The surface of the coating has no obvious pores or irregularities, making the surface of the coating smoother, resulting in a contact angle value of 126.1. Under high-temperature conditions, the unsaturated fatty acids in Tung oil may undergo oxidation due to oxygen, and volatile organic solvents may be released [57], accelerating the deterioration of the pigment coating surface, resulting in a decrease in the contact angle value of the pigment specimen to  $110.7^\circ$  at  $40^\circ\text{C}$ . These data emphasize the protective effect of lacquer and pigment coatings on wood substrates, while the ash coating as a transitional structure does not provide protection.

### 3.5. Glossiness of the Black Lacquer and Oil Pigment Coatings

Glossiness is an important indicator for evaluating surface physical property changes in color coatings [58]. The gloss loss of the lacquer specimens under wet and dry cycling conditions is shown in Figure 9. With an increase in the number of cycles, the glossiness damage to the lacquer specimens gradually intensifies. This is due to the microstructural changes on the surface of the lacquer film caused by the wet and dry cycles [59], resulting in an increase in its surface roughness, leading to a decrease in its glossiness. After five wet and dry cycles under  $40^\circ\text{C}$  conditions, the gloss loss rate of the black lacquer specimen reached up to 6.83%, indicating that the temperature accelerated the aging effect of moisture on the lacquer film. The gloss loss rate is directly proportional to the temperature, with the gloss loss rate at  $40^\circ\text{C}$  significantly higher than those at  $30^\circ\text{C}$  and  $20^\circ\text{C}$ . This may be because the high temperature promotes oxidation reactions on the surface of the black lacquer [60], leading to the formation of oxides and consequently causing a decrease in glossiness.

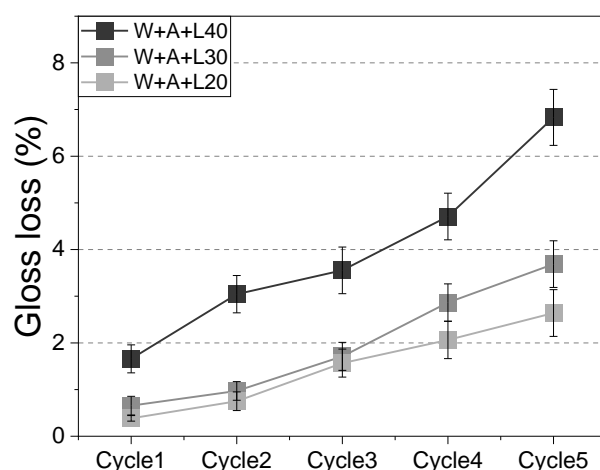


**Figure 9.** Gloss loss of black lacquer specimen under wet and dry cycling conditions.

As the experimental conditions were designed to simulate temperature and humidity variations in natural environments with a moderate acceleration intensity, and considering that the glossiness of the pigment specimens was inherently low, significant differences in the glossiness values after the aging of the pigment specimens were not observed.

#### 4. Conclusions

In conclusion, using alternating wet and dry cycle experiments on four types of Coromandel coatings, namely no coating, a pig blood–ash layer, a black lacquer layer, and an oil pigment layer, the protective effects of these coatings on the wood substrate were studied. The research findings are as follows:

- (1) Under wet and dry cycle conditions, all four types of Coromandel specimens experienced moisture expansion and contraction. The results indicate that under conditions of 40 °C and 30% RH, the dry shrinkage rate of the Coromandel specimens was maximal, while under conditions of 20 °C and 80% RH, the wet expansion rate was maximal. The ash, lacquer, and pigment layers all provided a certain degree of protection to the wood substrate. From the radial moisture expansion rate, it could be seen that after five wet cycles, the radial moisture expansion rate of the lacquer specimens was 0.079%, which was 23.8% of the radial moisture expansion rate of the wood specimens, indicating the best protective effect.
- (2) Specimen type significantly influences the moisture swelling and dry shrinkage rates, while temperature significantly affects the dry shrinkage rates. Across different experimental conditions, changes in the mass of the Coromandel specimens align with their dimensional changes, indicating that moisture absorption and desorption are the primary reasons for dimensional changes.
- (3) With an increase in the number of wet and dry cycles, the adhesion of the Coromandel specimens showed a slight decrease. The ash layer was identified as a weak interface, representing the weakest interface layer between the ash layer and the wood layer. After wet and dry cycles at 40 °C, the adhesion strength of the Coromandel specimens decreased the most, with the ash specimens decreasing by 7.2%, the lacquer specimens by 3.2%, and the pigment specimens by 4.5%.
- (4) After wet and dry cycles, the surface glossiness and hydrophobicity of the Coromandel coatings decreased to a certain extent with an increasing number of cycles, further exacerbated by induced temperature. Following wet and dry cycles at three different temperatures, the contact angle of the lacquer layers changed by less than 5%, with their contact angle values exceeding 120°, while the loss of glossiness reaches up to 6.83%.

In summary, this study provides a comprehensive understanding of the complex interactions between Coromandel coatings, wood substrates, and environmental conditions. These findings emphasize the importance of temperature and humidity in the stability and degradation of Coromandel coatings. Furthermore, future research could delve deeper into the durability and protective effects of different types of Coromandel coatings, as well as conducting a more thorough analysis of the mechanisms according to which various environmental factors affect Coromandel lacquer artifacts.

**Author Contributions:** Conceptualization, W.L. and X.L.; software, W.L.; investigation, A.M.V.; data curation, L.Z.; writing—original draft preparation, W.L.; writing—review and editing, X.L.; project administration, J.L.; funding acquisition, J.L. All authors have read and agreed to the published version of the manuscript.

**Funding:** Funding was received from the Ministry of Education’s Humanities and Social Sciences Research Fund project (21YJC760017), China.

**Data Availability Statement:** Data is contained within the article.

**Acknowledgments:** The authors would like to thank the College of Furnishings and Industrial Design, Nanjing Forestry University, for facilitating the experimental conditions.

**Conflicts of Interest:** The authors declare no conflicts of interest.

## References

1. Wu, M.; Zhang, B.; Jiang, L.; Wu, J.; Sun, G. Natural lacquer was used as a coating and an adhesive 8000 years ago, by early humans at Kuahuqiao, determined by ELISA. *J. Archaeol. Sci.* **2018**, *100*, 80–87. [[CrossRef](#)]
2. Zhai, K.; Sun, G.; Zheng, Y.; Wu, M.; Zhang, B.; Zhu, L.; Hu, Q. The earliest lacquerwares of China were discovered at Jingtoushan site in the Yangtze River Delta. *Archaeometry* **2021**, *64*, 218–226. [[CrossRef](#)]
3. Yuming, S. *Explanatory Commentary on the 'Xiu Shi Lu' of Jianjia Tang*; Taiwan Commercial Press: Taipei, Taiwan, 1974.
4. Shixiang, W. *Explanatory Commentary on Xiu Shi Lu*; Sanlian Bookstore for Life, Reading, and New Knowledge: Beijing, China, 2013.
5. Bei, C. *Illustrated Explanation of Xiu Shi Lu*; Shandong Pictorial Publishing House: Jinan, China, 2021.
6. Wenfu, D. *A Study of Ancient Chinese Lacquered Furniture: Evidence from the 10th to 18th Centuries*; Cultural Relics Publishing House: Beijing, China, 2012.
7. Brugier, N. *Les laques de Coromandel*; La Bibliothèque des Arts: Lausanne, Switzerland, 2015.
8. Fei, N. Flocks of Birds Flying Westward: The Western Transmission of Chinese Kuancai Lacquer Screens—Starting from the Exhibition of Qing Kangxi's 'Bai Niao Chao Feng' Twelve-Panel Lacquer Screen with Black Lacquer and Polychrome at the Muen-scher Lackkunst Museum, Germany. In Proceedings of the Guangzhou Cultural and Creative Industry Exposition; Guangzhou Cultural Museum: Guangzhou, China, 2017; pp. 112–117+194–228.
9. Zhu, Y.; He, J.; Zhang, L. Restoration of Coromandel Lacquer Screens in Jinhua Museum. In Proceedings of the ICOM-CC 20th Triennial Conference, Valencia, Spain, 18–22 September 2023.
10. Qu, S.; Ju, P.; Zuo, Y.; Zhao, X.; Tang, Y. The effect of various cyclic Wet-Dry exposure cycles on the Failure Process of Organic Coatings. *Int. J. Electrochem. Sci.* **2019**, *14*, 10754–10762. [[CrossRef](#)]
11. Wang, Q.; Feng, X.; Liu, X. Advances in historical wood consolidation and conservation materials. *Bioresources* **2023**, *18*, 6680–6723. [[CrossRef](#)]
12. Cheng, J. *Wood Science*; China Forestry Publishing House: Beijing, China, 1985.
13. Gereke, T.; Anheuser, K.; Lehmann, E.; Kranitz, K.; Niemz, P. Moisture behaviour of recent and natural aged wood. *Wood Res.* **2011**, *56*, 33–42.
14. Bai, R.; Wang, W.; Chen, M.; Wu, Y. Study of ternary deep eutectic solvents to enhance the bending properties of ash wood. *RSC Adv.* **2024**, *14*, 8090–8099. [[CrossRef](#)] [[PubMed](#)]
15. Liu, J.; Ji, Y.; Lu, J.; Li, Z. Mechanical Behavior of Treated Timber Boardwalk Decks under Cyclic Moisture Changes. *J. Korean Wood Sci. Technol.* **2022**, *50*, 68–80. [[CrossRef](#)]
16. Wang, J.; Cao, X.; Yang, Q.; You, H.; Qi, X. Experimental Study on Accelerating Aging of Larch Glued with Dry-Wet Cycling. *J. Hunan Univ.* **2022**, *50*, 156–164.
17. Garcia Esteban, L.; Gril, J.; de Palacios de Palacios, P.; Guindeo Casasús, A. Reduction of wood hygroscopicity and associated dimensional response by repeated humidity cycles. *Ann. For. Sci.* **2005**, *62*, 275–284. [[CrossRef](#)]
18. Yang, R.; Li, K.; Wang, L.; Bornert, M.; Zhang, Z.; Hu, T. A micro-experimental insight into the mechanical behavior of sticky rice slurry-lime mortar subject to wetting-drying cycles. *J. Mater. Sci.* **2016**, *51*, 8422–8433. [[CrossRef](#)]
19. Kesel, W.D.; Dhondt, G. *Coromandel Lacquer Screens*; Art Media Resources Ltd.: Chicago, IL, USA, 2002.
20. Qing, Y.; Liu, M.; Wu, Y.; Jia, S.; Wang, S.; Li, X. Investigation on stability and moisture absorption of superhydrophobic wood under alternating humidity and temperature conditions. *Results Phys.* **2017**, *7*, 1705–1711. [[CrossRef](#)]
21. Cha, J.K. Effect of Cyclic Moisture Content Changes on Shrinkage and Thermal Conductivity in Domestic *Quercus acutissima* Carr. and *Larix kaempferi* Carr. *J. Korean Wood Sci. Technol.* **2002**, *30*, 41–50.
22. Čermák, P.; Rautkari, L.; Horáček, P.; Saake, B.; Rademacher, P.; Sablik, P. Analysis of Dimensional Stability of Thermally Modified Wood Affected by Re-Wetting Cycles. *Bioresources* **2015**, *10*, 3242–3253. [[CrossRef](#)]
23. *ASTM G154*; Standard Practice for Operating Fluorescent Ultraviolet (UV) Lamp Apparatus for Exposure of Non-Metallic Materials. MICOM Inc.: Baie-d'Urfé, QC, Canada, 2023.
24. *ASTM D1037*; The ASTM International site is currently unavailable for scheduled maintenance. ASTM: West Conshohocken, PN, USA, 2020.
25. Akahoshi, H.; Obataya, E. Effects of wet-dry cycling on the mechanical properties of *Arundo donax* L. used for the vibrating reed in woodwind instruments. *Wood Sci. Technol.* **2015**, *49*, 1171–1183. [[CrossRef](#)]
26. Biblis, E.J.; Lee, W.C. *Effect of Repeated Humidity Cycling on Properties of Southern Yellow Pine Particleboard*; Auburn University: Auburn, AL, USA, 1975; pp. 1–12.
27. Yang, Z.; Zhang, M.; Liu, Y.; Lv, B.; Sun, X. Review of Literature on the Failure of Wood Coating. *Sci. Silvae Sin.* **2014**, *50*, 127–133.
28. Na, B.; Wang, H.; Ding, T.; Lu, X. Influence of Wet and Dry Cycle on Properties of Magnesia-Bonded Wood-Wool Panel. *Wood Res.* **2020**, *65*, 271–282. [[CrossRef](#)]
29. Haoliang, H. Methods of Refining Chinese Lacquer and Categories of Refined Chinese Lacquer. *Chin. Raw Lacq.* **2003**, *2*, 19–30. [[CrossRef](#)]
30. Miklin-Kniefacz, S.; Pitthard, V.; Parson, W.; Berger, C.; Stanek, S.; Griesser, M.; Kučková, Š.H. Searching for blood in Chinese lacquerware: Zhū xiě huī 豬血灰. *Stud. Conserv.* **2016**, *61*, 45–51. [[CrossRef](#)] [[PubMed](#)]
31. Hwang, I.S.; Park, J.H.; Kim, S.-C. A Study on the Optical Characteristics According to the Lacquer Drying Conditions for the Conservation of Lacquerwares. *J. Korean Wood Sci. Technol.* **2018**, *46*, 610–621. [[CrossRef](#)]

32. Zheng, L.P.; Wang, L.Q.; Zhao, X.; Yang, J.L.; Zhang, M.X.; Wang, Y.F. Characterization of the materials and techniques of a birthday inscribed lacquer plaque of the qing dynasty. *Herit. Sci.* **2020**, *8*, 10. [[CrossRef](#)]
33. He, L. *Analysis and Identification of Ancient Chinese Polychromy*; Science Publishing House: Beijing, China, 2017.
34. Yang, L.; Zheng, J.T.; Huang, N. The Characteristics of Moisture and Shrinkage of *Eucalyptus urophylla* × *E. Grandis* Wood during Conventional Drying. *Materials* **2022**, *15*, 3386. [[CrossRef](#)]
35. Chang, B. *Collection of Chinese Traditional Crafts. Natural Lacquer Painting*; China Science and Technology Press: Beijing, China, 2018.
36. GB/T 1927.4-2021; Test Method for Physical and Mechanical Properties of Flawless Small Specimens of Wood. State Administration for Market Regulation and the Standardization Administration of the People's Republic of China: Beijing, China, 2021.
37. Zhan, T.; Jiang, T.; Shi, T.; Peng, H.; Lyu, J. Heat Modification of Chinese Fir Wood Catalyzed by Fly Ash under Mild Temperature. *ACS Sustain. Chem. Eng.* **2023**, *11*, 14487–14496. [[CrossRef](#)]
38. Tao, M.; Liu, X.; Xu, W. Effect of the Vacuum Impregnation Process on Water Absorption and Nail-Holding Power of Silica Sol-Modified Chinese Fir. *Forests* **2024**, *15*, 270. [[CrossRef](#)]
39. GB/T 5210-2006; Color and Varnish Pull-off Method Adhesion Test. The General Administration of Quality Supervision, Inspection and Quarantine and the Standardization Administration of the People's Republic of China: Beijing, China, 2006.
40. ASTM D523-2014; Standard Test Method for Specular Gloss. ASTM International, W.C.: West Conshohocken, PA, USA, 2014.
41. GB/T 4893.6-2013; Physical and Chemical Properties Test of Furniture Surface Paint Film. Standardization Administration of the People's Republic of China: Beijing, China, 2013.
42. Liu, Y.; Zhao, G. *Wood Science*; China Forestry Press: Beijing, China, 2012.
43. Liu, H.; Ke, M.; Zhou, T.; Sun, X. Effect of Samples Length on the Characteristics of Moisture Transfer and Shrinkage of *Eucalyptus urophylla* Wood during Conventional Drying. *Forests* **2023**, *14*, 1218. [[CrossRef](#)]
44. Rowell, R.M.; Youngs, R.L. *Dimensional Stabilization of Wood in Use*; Forest Products Laboratory: Madison, WI, USA, 1981.
45. Inagaki, T.; Yonenobu, H.; Tsuchikawa, S. Near-infrared spectroscopic monitoring of the water adsorption/desorption process in modern and archaeological wood. *Appl. Spectrosc.* **2008**, *62*, 860–865. [[CrossRef](#)] [[PubMed](#)]
46. Obataya, E.; Ohno, Y.; Tomita, B. Changes in the vibrational properties of wood coated with urushi [Japanese] lacquer during moisture adsorption and desorption. *J. Jpn. Wood Res. Soc.* **2001**, *47*, 440–446.
47. Hastie, T.; Tibshirani, R.; Friedman, J.H. *The Elements of Statistical Learning: Data Mining, Inference, and Prediction*; Springer: Berlin/Heidelberg, Germany, 2009; Volume 2.
48. Lee, C.-J.; Lee, N.-H.; Park, M.-J.; Park, J.-S.; Eom, C.-D. Effect of Reserve Air-Drying of Korean Pine Heavy Timbers on High-temperature and Low-humidity Drying Characteristics. *J. Korean Wood Sci. Technol.* **2014**, *42*, 49–57. [[CrossRef](#)]
49. Thei, J. *Artificial Ageing of Japanese Lacquerware and Comparison of Conservation Treatments for Photodegraded Japanese Lacquer Surfaces*; Imperial College London: London, UK, 2012.
50. Montazeri, S.; Ranjbar, Z.; Rastegar, S.; Deflorian, F. A new approach to estimates the adhesion durability of an epoxy coating through wet and dry cycles using creep-recovery modeling. *Prog. Org. Coat.* **2021**, *159*, 106442. [[CrossRef](#)]
51. Volkmer, T.; Glaunsinger, M.; Mannes, D.; Niemz, P.J.B. Investigations on the influence of moisture on the adhesion strength of surface coating of wood. *Bauphysik* **2014**, *36*, 337–342. [[CrossRef](#)]
52. Zou, W.; Yeo, S.Y. Characterization of the Influence of the Particle Size of Pigments on Proteinaceous Binders Used in Ancient Wall Paintings Following Photo and Thermal Ageing. *Anal. Lett.* **2024**, *57*, 1078–1091. [[CrossRef](#)]
53. McSharry, C.; Faulkner, R.; Rivers, S.; Shaffer, M.S.P.; Welton, T. The chemistry of East Asian lacquer: A review of the scientific literature. *Stud. Conserv.* **2013**, *52*, 29–40. [[CrossRef](#)]
54. Gholamiyan, H.; Tarmian, A. Weathering Resistance of Poplar Wood Coated by Organosilane Water Soluble Nanomaterials. *Drv. Ind.* **2018**, *69*, 371–378. [[CrossRef](#)]
55. Zhang, F.L. *Chinese Lacquer Craft and Lacquerware Conservation*; Science Press: Beijing, China, 2010.
56. Na, W.; Ling, H. Analysis of Tung Oil Aging and Research on the Influence of Pigments on Its Aging. In Proceedings of the 9th Annual Academic Conference of the China Institute of Cultural Relics Preservation Technology, Chongqing, China, 22 November 2016; pp. 435–443.
57. dePolo, G. *Chemical and Mechanical Properties of Drying Oils During Polymerization*; Northwestern University: Evanston, IL, USA, 2023.
58. Peng, X.; Zhang, Z.; Wang, B.; Du, W. Research on the Aging Properties of Exterior Wood Coatings. In Proceedings of the 2012 International Conference on Biobase Material Science and Engineering, Changsha, China, 21–23 October 2012; pp. 121–126.
59. Shimadzu, Y.; Kawanobe, W. Deterioration Phenomena of Urushi Films: Combined Effects of Ultraviolet Radiation and Water. *Shikizai* **2003**, *76*, 385–390.
60. Liu, X. *Modelling the Mechanical Response of Japanese Lacquer (Urushi) to Varying Environmental Conditions*; Loughborough University: Loughborough, UK, 2012.

**Disclaimer/Publisher's Note:** The statements, opinions and data contained in all publications are solely those of the individual author(s) and contributor(s) and not of MDPI and/or the editor(s). MDPI and/or the editor(s) disclaim responsibility for any injury to people or property resulting from any ideas, methods, instructions or products referred to in the content.